Eur. Phys. J. D (2016) 70: 258
DOI: 10.1140/epjd/e2016-70212-8

THE EUROPEAN PHYSICAL JOURNAL D

Regular Article

Buffer gas-assisted four-wave mixing resonances in alkali vapor excited by a single cw laser

Svetlana Shmavonyan[1], Aleksandr Khanbekyan[1], Alen Khanbekyan[2], Emilio Mariotti[3], and Aram V. Papoyan[1,a]

[1] Institute for Physical Research, NAS of Armenia, 0203 Ashtarak, Armenia
[2] Department of Physics and Earth Sciences, University of Ferrara, via Saragat 1, 44122 Ferrara, Italy
[3] Department of Physical Sciences, Earth and Environment, University of Siena, via Roma 56, 53100 Siena, Italy

Received 22 March 2016 / Received in final form 30 May 2016
Published online 6 December 2016 –

Abstract. We report the observation of a fluorescence peak appearing in dilute alkali (Rb, Cs) vapor in the presence of a buffer gas when the cw laser radiation frequency is tuned between the Doppler-broadened hyperfine transition groups of an atomic D_2 line. Based on steep laser radiation intensity dependence above the threshold and spectral composition of the observed features corresponding to atomic resonance transitions, we have attributed these features to the buffer gas-assisted four-wave mixing process.

1 Introduction

Nonlinear optical processes in gaseous media, in particular alkali metal vapor, induced under excitation by intense pulsed (quasi)resonant laser radiation were extensively studied since invention of lasers. For the case of conventional low-power cw laser excitation, the intensities drop down by many orders of magnitude, but on the other hand the much narrower spectral linewidth of cw lasers makes favorable resonant interaction with atomic media. As a result, some nonlinear processes become observable with cw excitation.

Among these processes are hyper-Raman scattering [1], four-wave mixing [1–6], up-conversion [5], degenerate two-photon absorption [7], etc. Nonlinear optical processes in resonant gaseous media can be enhanced by some assisting mechanisms, in particular collisions with foreign (buffer) gas particles.

Addition of a buffer gas to the resonant gaseous atomic medium (in particular, alkali metal vapor) may result in several consequences. Firstly, it traps the alkali atoms preventing their escape from the laser beam, thus increasing the interaction time of individual atoms with laser radiation. Secondly, the high enough density of buffer gas causes homogeneous collisional broadening and shift of atomic transitions. These issues are discussed in many papers (see e.g. [8–11]). Thirdly, frequent elastic collisions of buffer gas particles with resonant atoms result in averaged uniform velocity distribution and thus homogeneous contribution from all the atoms in the interaction region. The averaging effect of such velocity-changing collisions reduces the Doppler broadening of isolated spectral lines and leads to collisional narrowing [12]. Another consequence was addressed in reference [13], where it was shown that the presence of H_2 buffer gas significantly modifies the intensity dependence of cesium resonant absorption and fluorescence, which was attributed to the resonant excitation-induced chemical reaction.

In reference [14] it was reported on observation of changes in the lineshape of Cs D_2 line in Ne-buffered cell, exhibiting a broad (about 10 GHz) wide spectral feature located between $F_g = 3 - F_e = 2, 3, 4$ and $F_g = 4 - F_e = 3, 4, 5$ hyperfine transition groups, which were attributed to laser-induced optical pumping and collisions in a buffer gas, and explained by a model dealing with ground state hyperfine levels population, Ne pressure broadening, and diffusion of atoms outside the laser beam.

Similar studies with different buffer gas (Cs + 20 Torr of H_2) have been performed in reference [15], revealing obvious distinctions: the above mentioned spectral feature (let us call it mid-resonance peak) was observable for the laser radiation intensity exceeding 3 mW/cm^2, with tenfold narrower spectral width and better spectral localization. The latter allowed us to suppose that there is yet another physical mechanism responsible for the observed behavior.

The present work is aimed at detailed experimental study of the mid-resonance features in fluorescence spectra, exploiting various interaction regimes and parameters (different types and pressures of buffer gas, wider intensity range), as well as implementing the spectral analysis of emitted radiation in order to clarify all the physical mechanisms responsible for formation of a mid-resonance peak. It should be noted that in this study we were interested in revealing new qualitative spectral features rather than absolute quantitative measurements and modeling of the results.

[a] e-mail: papoyan@ipr.sci.am

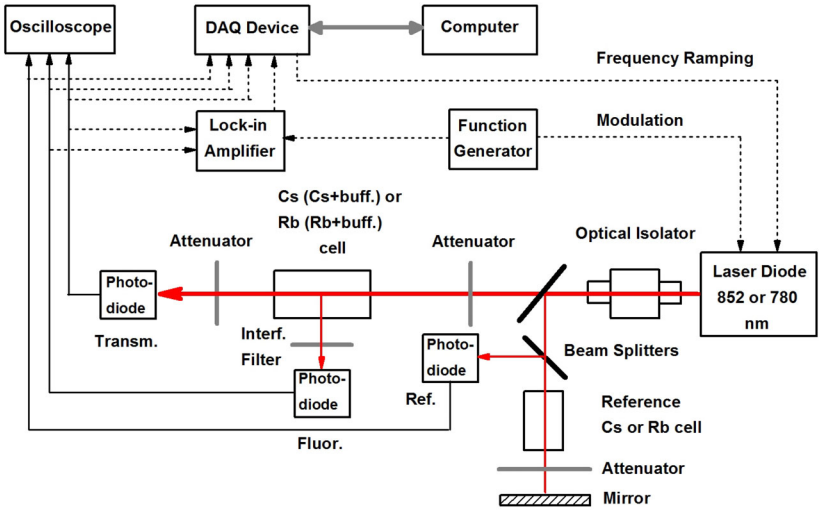

Fig. 1. Schematic diagram of experimental setup.

Table 1. The cells used in the experiment.

No.	Metal	Buffer gas	P_{buf} (Torr)
1	Cs	–	–
2	Cs	H_2	20
3	Rb	–	–
4	Rb	H_2	18
5	Rb	H_2	13
6	Rb	Ar	3.5
7	Rb	Ar	35
8	Rb	Ne	20

2 Experimental

Experimental measurements have been performed on two different setups. General schematic diagram of the setups is shown in Figure 1. The ⊘ = 1.5 to 3 mm linearly-polarized unfocused radiation beam of a solitary cw diode laser (wavelength 780 nm for Rb D_2 line or 852 nm for Cs D_2 line, with 2 to 25 MHz linewidth) was normally directed into one of the 30 to 80 mm-long sealed-off vapor cells containing rubidium or cesium listed in Table 1, without or with admixture of buffer gas at different pressures.

Most of the measurements were performed at room temperature (the number density of Rb and Cs atoms is $N_{\mathrm{Rb}} = 1.4 \times 10^{10}$ cm^{-3} and $N_{\mathrm{Cs}} = 7.55 \times 10^{9}$ cm^{-3} at 20 °C). The cell was placed in three pairs of mutually perpendicular Helmholtz coils canceling the ambient magnetic field. The laser frequency was linearly scanned without mode hopping in a spectral range of up to 25 GHz covering the Doppler-overlapped hyperfine transition groups of D_2 lines of rubidium ($5S_{1/2} - 5P_{3/2}$: ^{85}Rb $F_g = 2 - F_e = 1, 2, 3$ and $F_g = 3 - F_e = 2, 3, 4$; ^{87}Rb $F_g = 1 - F_e = 0, 1, 2$ and $F_g = 2 - F_e = 1, 2, 3$) or cesium ($6S_{1/2} - 6P_{3/2}$: ^{133}Cs $F_g = 3 - F_e = 2, 3, 4$ and $F_g = 4 - F_e = 3, 4, 5$). Linear scanning of the laser radiation frequency was realized by means of internal or external triangular modulation, slow enough to assure development of a steady-state interaction regime. A fraction of the laser radiation was branched to the saturation absorption setup with an auxiliary cell with pure Rb (Cs) serving as a frequency reference.

Three photodiodes followed by operation amplifiers were used to detect the fluorescence, transmission, and reference spectra. Fluorescence was measured at 90° to the direction of laser propagation, covering solid angle of ≈0.1 srad. The range of variation of the laser radiation intensity was limited by the unattenuated laser power from above, and by the signal-to-noise ratio of fluorescence from below. Focusing the laser beam could increase the maximum intensity, but in this case the interaction conditions (time of flight, intensity, number of interacting atoms) would be dependent on propagation distance, thus complicating interpretation of the results.

Most of the measurements were carried out implementing computer control of laser radiation frequency and data acquisition using a DAQ board. For some measurements, frequency modulation of the laser radiation followed by lock-in detection of optical signals was utilized.

3 Results and discussion

3.1 Fluorescence excitation spectra

No mid-resonance peak was observed in Rb and Cs vapor cells without admixture of a buffer gas (cells Nos. 3 and 1) for all the exploited range of the laser radiation power (up to 50 mW). In contrast, this spectral feature was observable already at 0.2 mW (for Cs) or 2 mW (for Rb) in buffered cells. The magnitude and spectral width of the mid-resonance peak are strongly dependent on the type and pressure of a buffer gas, as well as laser radiation intensity. We present below typical spectra measured at different experimental conditions.

Fluorescence excitation spectra recorded in a room temperature Rb cell with addition of 13 Torr of hydrogen (cell No. 5) at 8 values of the laser radiation power P_L ranged between 1 mW and 30 mW are shown in the left

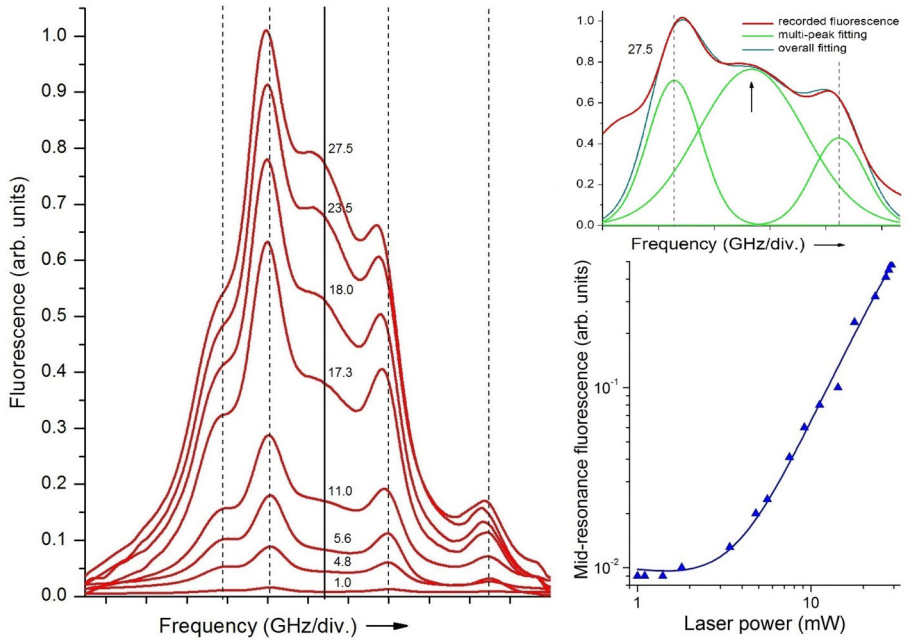

Fig. 2. Left graph: fluorescence excitation spectra of Rb with 13 Torr of H_2 (cell No. 5) for eight values of P_L (marked in mW for each trace); vertical lines: positions of hyperfine transition groups (dashed, left to right): ^{87}Rb $F_g = 2 - F_e = 1, 2, 3$, ^{85}Rb $F_g = 3 - F_e = 2, 3, 4$, ^{85}Rb $F_g = 2 - F_e = 1, 2, 3$, ^{87}Rb $F_g = 1 - F_e = 0, 1, 2$; spectral feature appearing at mid-resonance position for high laser intensity (solid). Right graph: dependence of mid-resonance signal magnitude on the laser power determined from multi-line fitting (upper inset, see text).

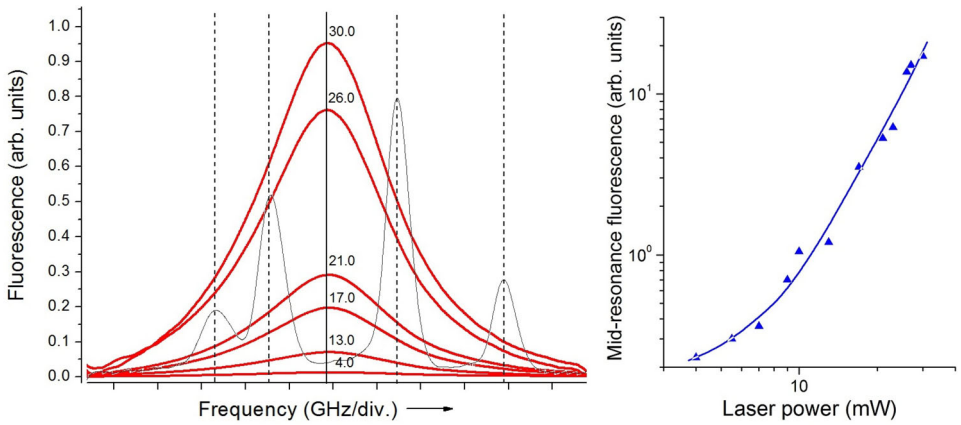

Fig. 3. Left graph: fluorescence excitation spectra of Rb with 35 Torr of Ar (cell No. 7) for six values of P_L (marked in mW for each trace); vertical lines: positions of hyperfine transition groups (dashed); spectral feature appearing at mid-resonance position for high laser intensity (solid). Right graph: dependence of mid-resonance signal on the laser power.

graph of Figure 2. It is clearly seen that a mid-resonance peak located at half-sum frequency of transitions $F_g = 2 - F_e = 1, 2, 3$ and $F_g = 3 - F_e = 2, 3, 4$ of ^{85}Rb develops in spectra as the laser intensity increases. Dependence of the magnitude of mid-resonance fluorescence on the laser radiation power is presented in the right graph of Figure 2, exhibiting threshold-type nonlinear course. A three peak fitting was used to extract the correct magnitude value from the highly overlapped envelope, as is shown on the upper inset of Figure 2 for $P_L = 27.5$ mW. The fitted linewidths of the three peaks were kept invariable for all the spectra.

Results of the same study done for another buffer gas (argon) at higher pressure (35 Torr) with otherwise identical experimental conditions are presented in Figure 3. One can see that qualitatively similar behavior (namely, mid-resonance fluorescence peak) is observed. The significant distinctions are its overall higher magnitude and much larger spectral width, which completely wipes off hyperfine resonance transitions.

The difference in spectral behavior observed in Figures 2 and 3 (notably, absence of the resonant fluorescence lines and wider linewidth of mid-resonance fluorescence in Fig. 3) should be partly attributed to the type of a buffer

gas (different collisional cross-sections), but mainly to the buffer gas pressure. Thus, the spectra recorded for the case of Rb with addition of 3.5 Torr of Ar (cell No. 6), are similar to those presented in Figure 2. Qualitatively the same behavior was observed also in the experimental graphs of [14] for the case of Cs with admixture of Ne at 1, 5, and 50 Torr: the resonance fluorescence peaks become almost unpronounced already for 5 Torr Ne pressure and 120 mW/cm^2 intensity. In the conditions of Figure 3, the lowest laser radiation intensity for 4 mW $\oslash$ = 1.5 mm beam is ≈150 mW/cm^2, and the buffer gas pressure is 7 times higaher, so the conditions of hiding the resonance fluorescence are more favorable.

Suppression of resonant fluorescence with the increase of laser intensity was addressed in reference [13]. For the slow scanning allowing establishment of a steady-state radiation-atom interaction and high radiation intensity, the optical depopulation pumping towards the second (inactive) ground state hyperfine sublevel becomes more effective, while in the buffer gas ambience there is no efficient mechanism of recovering the population of the initial ground sublevel, since there are no atom-wall spin-flip collisions available in the case of pure vapor.

For the case of ^{133}Cs the hyperfine splitting of the ground state is three-fold larger as compared with ^{85}Rb (9192.3 GHz vs. 3035.7 GHz). Thus, possible contribution of Doppler broadening (∼0.5 GHz) discussed in reference [14] is expected to be less determinative. In spite of this, the mid-resonance fluorescence is observed here more clearly, even at lower laser radiation intensity. Experimental data for this case can be found in reference [15].

We should note that the mid-resonance feature is observable in H_2-buffered Cs cell also in the transmission spectrum in the same experimental conditions, as a dip appearing when the laser radiation is tuned to the half-sum frequency of hyperfine transition groups $6S_{1/2}$, $F_g = 3 - 6P_{3/2}$, $F_e = 2, 3, 4$ and $6S_{1/2}$, $F_g = 4 - 6P_{3/2}$, $F_e = 3, 4, 5$ [15]. The spectral width of this dip (∼1 GHz) is comparable with the Doppler-overlapped hyperfine transition groups (for individual transition, the Doppler broadening of an individual hyperfine transition is 380 MHz at room temperature). For detection of the low-intensity fluorescence spectra, as well as low-amplitude spectral features in transmission spectra, when overall transmission approaches 100%, we have implemented frequency modulation and lock-in detection technique.

We have also performed a set of measurements to study dependence of the fluorescence spectral profile on the vapor density. An example of these measurements is presented in Figure 4 for the case of a Rb cell filled with 20 Torr of neon (cell No. 8), keeping the laser power invariable.

As is expected, the fluorescence signal increases and broadens with vapor density. When N_{Rb} exceeds 10^{12} cm^{-3}, self-absorption of the emerged radiation occurs in the cell outside the laser beam, resulting in dips centered at the hyperfine transitions. Besides, self-absorption is observed also for the mid-resonance fluorescence (see trace 7 in Fig. 5), which was also proven by a multi-peak fitting analysis. The latter indicates that the mid-resonance fluorescence in the excitation spectrum can be attributed to resonance emission. Below we present the results of its spectral analysis.

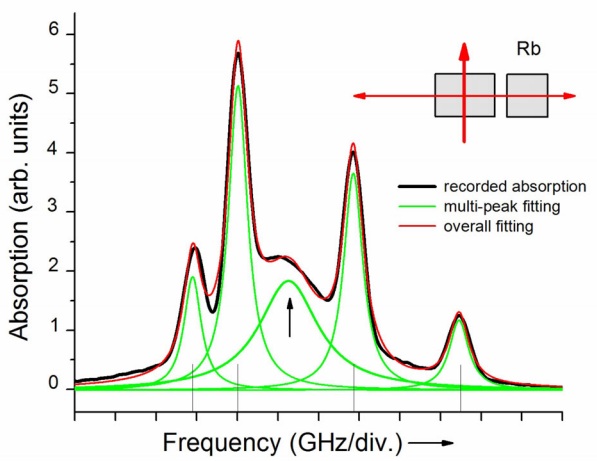

Fig. 4. Black trace: net absorption of fluorescence signal (cell No. 4, P_L = 21 mW) in the second cell with pure Rb (see text). Green traces: multi-peak fitting of the recorded spectrum; red trace: overall fitted spectrum. Vertical dashes indicate positions of hyperfine transition groups (see text); the arrow marks position of the mid-resonance peak.

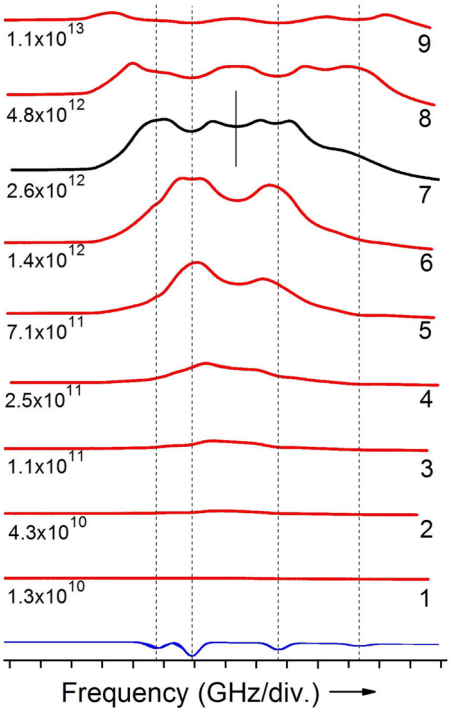

Fig. 5. Fluorescence excitation spectra of Rb with 20 Torr of Ne (cell No. 8) measured with P_L = 15 mW at 9 temperature values from 25 to 113 °C; corresponding vapor densities are indicated in cm^{-3}.

3.2 Spectral analysis of emitted radiation

The mid-resonance fluorescence peak recorded in our experiment appears in the excitation spectra. Additional spectral analysis of the emitted radiation is needed to identify the frequency of the fluorescence emerging from the cell when the laser is tuned mid way (half-sum frequency) between the two hyperfine transitions.

Additional measurements have been implemented for the spectral analysis of the mid-resonance fluorescence. First, we have used a narrow-band filter (central wavelength 780 nm, bandwidth 2 nm) to make sure that the wavelength of emerging fluorescence feature is within the spectral range of Rb D_2 line. The spectral resolution of conventional spectrometers is not high enough to distinguish components with sub-GHz separation. On the other hand, sensitivity of the commercial scanning Fabry-Pérot cavity destined for determination of laser radiation frequency was not sufficient to record weak fluorescence signal. To overcome these restrictions, vapor cells were used as spectral devices.

The first measurement was done with the following configuration. The laser radiation passed along the cell axis, and two identical photodetectors were placed in the transverse direction to record fluorescence in opposite directions, on equal distances from the cell. In one of symmetric wings, an auxiliary cell with pure Rb (with no buffer gas) was installed between the main cell and photodetector (see the inset in Fig. 4). By subtracting the spectrum recorded by the right detector from the one recorded by the left detector, we derive the net absorption spectrum of the fluorescence in the auxiliary cell. This spectrum is plotted in Figure 4 together with fitted curves. It is clearly seen that the fluorescence emerging from the buffered cell when the laser is tuned to mid-resonance position gets absorbed in the auxiliary cell. This indicates that the fluorescence occurs on resonant hyperfine transitions of D_2 line.

The second check was done in a modified configuration, without an auxiliary cell: a single photodetector was placed on one side of the same buffered Rb cell, faced normally to the laser beam direction (see the inset in Fig. 6). The first fluorescence measurement (case 1) was done when the laser beam passed close to the cell generatrix facing the photodetector. The second measurement (case 2) was done when the cell was translated so that the laser beam passed close to the opposite generatrix. The recorded spectra (1, 2) and their difference showing the net self-absorption signal (3) are presented in Figure 6 for high and low laser radiation power. Also here one can see that resonant absorption of mid-resonance fluorescence occurs in the case of high excitation intensity.

3.3 Buffer gas-assisted four-wave mixing

Based on experimental observations presented above, one may conclude that the mid-resonance peak in fluorescence signal is caused by a degenerate four-wave parametric process schematically depicted in Figure 7. Two pathways of such process provide linkage of two ground state hyperfine sublevels (1 and 2) with the Doppler-overlapped excited state sublevels (3) by the same mid-resonance laser radiation (ν_L) and resonant atomic emissions (ν_{31} and ν_{32}).

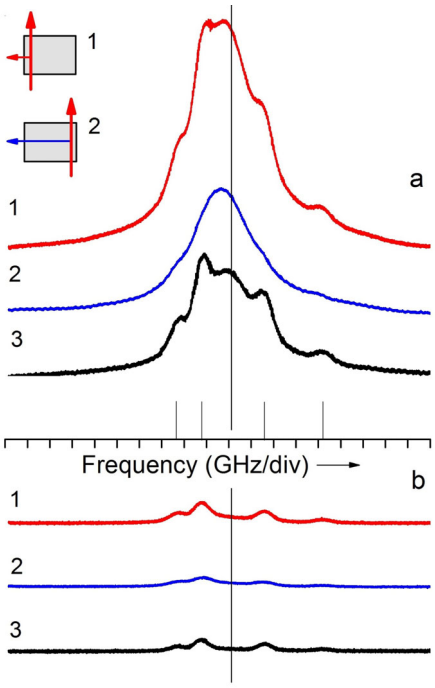

Fig. 6. Fluorescence excitation spectra (cell No. 4) recorded without (1) and with (2) self-absorption in the cell, and their difference (net absorption signal, 3). P_L = 30 mW (a) and 1.1 mW (b). Vertical dashes indicate positions of hyperfine transition groups; vertical line marks position of the mid-resonance peak appearing at high laser intensity (see text for details).

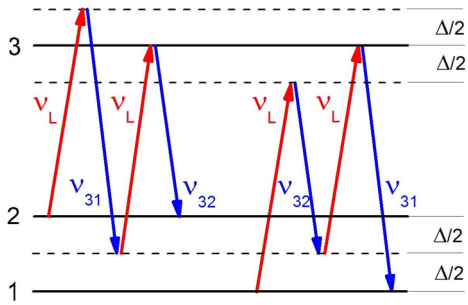

Fig. 7. Diagram of two pathways of the four-photon parametric process in a 3-level atomic system.

As is seen from Figure 7, a four-wave mixing assisted by resonant emission on atomic transitions can occur only when $\nu_L = (\nu_{31} + \nu_{32})/2$.

The efficiency of this process at relatively low laser radiation intensities (the threshold intensity in Figures 2 and 3 is ≈110 mW/cm^2 corresponding to ≈2.5 mW power with ⌀ = 1.5 mm laser radiation beam) should be attributed to the resonant nature of the four-wave mixing process (Fig. 7), and narrow spectral linewidth of the laser

radiation. We should note that the low power value required to observe the mid-resonance fluorescence in our experiment is consistent with other experiments on four-wave mixing with cw lasers (e.g., 20 mW for the blue light generation in Ref. [5], and a few mW for the double-Λ scheme generation in Ref. [2]).

Addition of a non-resonant buffer gas to alkali metal vapor resonantly interacting with laser radiation plays dual role for this process. Firstly, the buffer gas with a density of particles exceeding the density of resonant atoms by several orders of magnitude suppresses thermal mobility of the resonant atoms due to frequent elastic collisions with buffer gas atoms (molecules), thus substantially increasing the interaction time of an individual atom with radiation field. Secondly, in buffer gas environment atoms undergo rapid succession of speed-changing elastic collisions, which results in uniform contribution from all the atoms. As a result, buffer gas stimulates the onset of four-wave mixing process, so that it becomes possible at mW level of the laser radiation power. Increasing the buffer gas pressure at invariable laser power enhances mid-resonance fluorescence, and simultaneously broadens its linewidth, as one can see comparing Figures 2 and 3.

Besides, the buffer gas can also assist the realization of a proper phase-matching condition favorable for the four-wave mixing, caused by variation of the refractive index of the vapor across the resonances [16]. Within the present study we failed to reveal changes in spatial profile of the transmitted radiation connected with ring-shape features inherent to four-wave mixing. This can be explained by weakness of the four-wave mixing signal compared to transmitted laser radiation, combined with proximity of their wavelengths, which makes it difficult to detect conical emission around transmitted laser beam. On the other hand, it is known that nonlinear mixing processes can yield coaxial emission in buffered vapor cells [6,16] thanks to phase matching assisted by buffer gas-induced refractive index changes.

4 Conclusions

We have experimentally studied the appearance of a "bright" resonance feature in Rb and Cs D_2 line, when the exciting laser radiation is tuned to the half-sum frequency of the transitions from the two hyperfine sublevels of the ground state. This "mid-frequency resonance" is absent in pure vapor cells up to at least 50 mW radiation power, but becomes observable in buffered vapor cells already at sub-mW-range power.

Based on the following findings: (i) absence of mid-resonance features in the cells without addition of buffer gas; (ii) threshold nature of the laser radiation intensity dependence of the mid-resonance amplitude, which significantly differs from the dependence for resonance transitions; (iii) resonant behavior of these spectral features appearing in the excitation spectra, we have concluded that the appearance of mid-resonance peculiarities in excitation spectrum has to be fully or partly attributed to a four-wave mixing process where two mid-resonance laser photons originate two photons on the D_2 line hyperfine transitions.

This process is strongly assisted by a buffer gas, which causes increase in the interaction time, as well as uniform contribution from all the atoms thanks to velocity-changing elastic collisions. As a result, four-wave mixing process becomes favorable in the same laser power range.

Unlike other known four-wave mixing processes under cw laser excitation reported so far, the one presented in our study develops within a three-level structure formed by the hyperfine sublevels of the same spectral line, and involves emission at resonant atomic transitions. The presence of two coherent pathways in resonance formation leading to generation of indistinguishable photon pairs and possibly dark resonances, can be of interest for quantum information applications.

Experimental evidences presented in this work are not yet supported by comprehensive theoretical modeling. We plan to perform theoretical treatment of the process, involving also laser-induced optical pumping and other related effects.

The authors are grateful to D. Sarkisyan, Yu. Malakyan, and T. Vartanyan for stimulating discussions. The research leading to these results has received funding from the European Union Seventh Framework Programme (FP7/2007-2013) under grant agreement No. 295264–COSMA.

References

1. M. Klug, S.I. Kablukov, B. Wellegehausen, Opt. Commun. **245**, 415 (2005)
2. R.M. Camacho, P.K. Vudyasetu, J.C. Howell, Nat. Photon. **3**, 103 (2009)
3. E. Brekke, L. Alderson, Opt. Lett. **38**, 2147 (2013)
4. B. Ai, D.S. Glassner, R.J. Knize, Phys. Rev. A **50**, 3345 (1994)
5. A.M. Akulshin, R.J. McLean, A.I. Sidorov, P. Hannafoed, Opt. Express **17**, 22861 (2009)
6. D.S. Glassner, R.J. Knize, Appl. Phys. Lett. **66**, 1593 (1995)
7. D. Krökel, D. Frölich, W. Klische, A. Feitish, H. Welling, Opt. Commun. **48**, 57 (1983)
8. S. Brandt, A. Nagel, R. Wynards, D. Meschede, Phys. Rev. A **56**, R1063 (1997)
9. C. Andreeva, S. Cartaleva, Y. Dancheva, V. Biancalana, A. Burchianti, C. Marinelli, E. Mariotti, L. Moi, K. Nasyrov, Phys. Rev. A **66**, 012502 (2002)
10. E.E. Mikhailov, I. Novikova, Yu.V. Rostovtsev, G.R. Welch, Phys. Rev. A **70**, 033806 (2004)
11. J. Belfi, V. Biancalana, S. Cartaleva, Y. Dancheva, E. Mariotti, L. Moi, K. Nasyrov, D. Slavov, P. Todorov, K. Vaseva, Acta Physica Polonica A **112**, 823 (2007)
12. P.L. Varghese, R.K. Hanson, Appl. Opt. **23**, 2376 (1984)
13. V. Chaltykyan, Yu. Malakyan, S. Shmavonyan, A. Papoyan, J. Phys. B **37**, 3735 (2004)
14. F. de Tomasi, M. Allegrini, E. Arimondo, G.S. Agarwal, P. Ananthalakshmi, Phys. Rev. A **48**, 3820 (1993)
15. S. Shmavonyan, A. Papoyan, Int. J. Mod. Phys.: Conf. Ser. **15**, 140 (2012)
16. I.V. Tomov, Phys. Lett. A **48**, 153 (1974)